

The translate of strongly abridged PhD thesis:
**ISOLATED LENTICULAR GALAXIES: PROPERTIES AND
EVOLUTION¹**

Ivan Yu. Katkov

*Lomonosov Moscow State University
Faculty of Physics, Sternberg Astronomical Institute
Universitetsky pr., 13, Moscow, 119991, Russia
katkov.ivan@gmail.com*

Abstract

This work is dedicated to investigation of galaxies that do not fit into a common scenario of galaxy formation – isolated lenticular galaxies. We have studied stellar populations and ionized gas content of a sample of 22 lenticular galaxies (among those 4 targets have appeared to be of erroneous morphological classification) by undertaking deep long-slit spectroscopy with the Russian 6-m telescope and with the Southern African Large Telescope (SALT). The obtained average ages of the stellar populations in bulges and discs covers a wide range between 1.5 and > 15 Gyr, that indicates the absence of distinct epoch of their stellar content formation. In contrast to galaxies in groups and clusters, the stellar population ages in bulges and discs of isolated lenticulars tend to be equal, that supports the inefficiency of the bulge rejuvenation in sparse environment. Almost all the lenses and rings possess intermediate ages of the stellar populations, within the range of 2 – 5 Gyr. By analyzing the emission-line spectra of galaxies, we have found that 13 out of 18 (72 ± 11 %) objects of our sample possess extended emission-line structures; among those, 6 galaxies (46 ± 14 %) demonstrate decoupled gas kinematics with respect to their stellar discs. We have found starforming off-nuclear regions in 10 galaxies; their gas oxygen abundances are nearly solar that implies tidal gas accretion from gas-rich dwarf satellites rather than accretion from cosmological large-scale structure filaments.

Subject headings: galaxies: elliptical and lenticular — galaxies: ISM — galaxies: kinematics and dynamics — galaxies: evolution.

Contents		4.2 Epoch and duration of formation stellar content	8
1 Introduction	1	4.3 Formation scenario	8
2 Sample of galaxies	2	5 Ionized gas	11
3 Observations and data analysis	2	5.1 Statistics of ionized gas decouplings . . .	11
3.1 6-m telescope BTA	2	5.2 Metallicity and origin of gas structures . .	11
3.2 SALT telescope	2	5.3 Luminosity-metallicity relation	12
3.3 Extraction of kinematics and stellar population properties	3	6 Conclusions	13
4 Stellar populations	3	1. Introduction	
4.1 Comparison of stellar populations for bulge, disc, lens/ring.	3	One of the central topics in current extragalactic astronomy is how galaxies form and how their properties change through cosmic times. This is a particularly difficult task if concerning lenticular galaxies since this class of objects show a diversity in their properties that goes beyond present day simulations.	
4.1.1 Bulges vs. discs	3	The standard scenario of formation of lenticular galaxies relates to transformation of spiral galaxies into lenticulars by dense environment effect: ram pressure in hot	
4.1.2 Disc substructures: lenses and rings	8		

¹The PhD thesis submitted to Lomonosov Moscow State University, Sternberg Astronomical Institute. PhD supervisor: Prof. Olga K. Sil'chenko (SAI MSU).

intracluster/intragroup medium (Gunn & Gott 1972; Quilis et al. 2000), gravitational tides and harassment (Byrd & Valtonen 1990; Moore et al. 1996), direct encounters of galaxies (Spitzer & Baade 1951; Icke 1985), starvation (Larson et al. 1980). However 15% of nearby field galaxies are lenticulars Naim et al. (1995), and there are examples of strictly isolated S0 Sulentic et al. (2006). The study of isolated lenticulars by using deep optical spectroscopy methods provided information not only for central part of galaxies but also for disc components, is important issue because it provides a crucial point for the testing of scenario formation of lenticulars at all.

2. Sample of galaxies

We have compiled our sample of isolated S0 galaxies basing on the approaches recently developed by the team of Igor Karachentsev, Dmitry Makarov, and co-authors (Special Astrophysical Observatory, Russia). Their group-finding algorithm that takes into account individual characteristics of galaxies has been already used to study the properties of isolated galaxies (Karachentsev et al. 2011), pair (Karachentsev & Makarov 2008), triple (Makarov & Karachentsev 2009) systems of galaxies and galaxy groups (Makarov & Karachentsev 2011). The LOG catalogue (“Local Orphan Galaxies”) of 520 extremely isolated galaxies has been presented in Karachentsev et al. (2011). However, LOG catalogue contains only 17 early type galaxies ($T < 0$). Thus, we composed list of 281 isolated S0 galaxies by slightly weakened the isolation criteria based on their approach. Using that list of galaxies we chosen targets for spectral observation. The details about selection criteria will be presented in Katkov et al. (2014b) and in the prepared paper with SALT data results (Katkov et al. in preparation).

3. Observations and data analysis

The observations of galaxies were carried out with 6-m Russian telescope operated by Special Astrophysical Observatory at the Russian Academy of Sciences (Nizhnij Arkhiz, Russia) as well as with Southern African Large Telescope (Sutherland, SA) during period 2011-2013 years under observation programs dedicated to studies of isolated S0s (P.I.: Olga K. Sil’chenko (SAI MSU), co-Is: Alexey Yu. Kniazev (SAAO, SAI MSU) and Ivan Yu. Katkov). We observed 22 targets, but subsequent analyses of Kormendy diagram reveals that 4 targets among 22 objects is ellipticals. So, the analysis of stellar populations and ionized gas carried out based only 18 galaxies.

3.1. 6-m telescope BTA

The spectral data for most galaxies were obtained using the new focal reducer SCORPIO-2 (Afanasiev & Moiseev 2011) maintained at the prime focus of the telescope. The grism VPHG1200@540 provides spectral resolution $\approx 4 \text{ \AA}$ in spectral range 3800 – 7300 \AA .

This spectral range included a set of strong absorption and emission features, making it suitable to study both internal stellar and gaseous kinematics and the stellar populations of the galaxy. The 1''-width slit was oriented along major axes of galaxies and was 6' in length, which provided the possibility of using the edge spectra to evaluate the sky background. The CCD chip E2V CCD42-90, with a format of 2048x4600, used in the 1x2 binning mode provided a spatial scale of $0''.357 \text{ pixel}^{-1}$ and a spectral sampling of $0.84 \text{ \AA pixel}^{-1}$.

The preliminary data reduction was identical to that applied to the lenticular galaxy NGC 7743 described in Katkov et al. (2011). Briefly, the primary data reduction was comprised of bias subtraction, flat-fielding, cosmic ray hit removal, and building the wavelength solution using the He-Ne-Ar arc-line spectra. To subtract the sky background, we invented a rather sophisticated approach. We constructed the spectral line-spread function (LSF) model varied along and across the wavelength direction by using the twilight spectrum (Katkov & Chilingarian 2011). The final stages of the long-slit spectra reduction were night sky spectrum subtraction taking into account the LSF variations, linearization, and accounting for spectral sensitivity variation using the spectrum of a spectrophotometrical standard star. The error frames were computed using the photon statistics and

3.2. SALT telescope

The observations were conducted with the Robert Stobie Spectrograph (Burgh et al. 2003; Kobulnicky et al. 2003) at Southern African Large Telescope. The long-slit spectroscopy mode of the RSS was used with a 1.25 arcsec slit width for the most of observations. The total time of one observational block with SALT is limited by the track-time of about an hour for our targets. For this reason and because SALT is a queue-scheduled telescope, most of our galaxies were observed more than once and all observations were done during different nights. The total time exposure per object between 0.5 and 3 hours. The slit was oriented along the major axis for all galaxies. The grating GR900 was used for our program to cover finally the spectral range of 3760 – 6860 \AA with a final reciprocal dispersion of $\approx 0.97 \text{ \AA pixel}^{-1}$ and FWHM spectral resolution of 4.7 – 4.8 \AA . The seeing during observations was in the range 1.5 – 3.0 arcsec. The RSS pixel scale is $0''.129$ and the effective field of view is 8' in diameter. We utilised a binning factors of 2 and 4 to give a final spatial sampling of $0''.258 \text{ pixel}^{-1}$ and $0''.516 \text{ pixel}^{-1}$ respectively. Spectrum of an Ar comparison arc was obtained to calibrate the wavelength scale after each observation as well as spectral flats were observed regularly to correct for the pixel-to-pixel variations. Spectrophotometric standard stars were observed during twilights, after observations of objects for the relative flux calibration.

Primary data reduction was done with the SALT science pipeline (Crawford et al. 2010). After that, the bias and gain corrected and mosaicked long-slit data were re-

duced in the way described in Kniazev et al. (2008). The accuracy of the spectral linearisation was checked using the sky line [O I] $\lambda 5577$; the RMS scatter of its wavelength measured along the slit is 0.04 \AA . The slit length is approximately $8'$, so sky spectra from the slit edges were used to estimate the background during the galaxy exposures.

3.3. Extraction of kinematics and stellar population properties

To derive information about stellar and ionized gas kinematics we first fitted the stellar absorption spectra by the PEGASE.HR high resolution stellar population models Le Borgne et al. (2004) convolved with a parametric line-of-sight (LOS) velocity distribution by applying NBURSTS full spectral fitting technique Chilingarian et al. (2007a,b). Before the minimization procedure, the model grid of stellar population spectra is convolved with the LSF. Multiplicative Legendre polynomials are also included to take into account possible internal dust reddening and residual spectrum slope variations due to the errors in the assumed instrument spectral response. Ionized-gas emission lines and remnants of the subtracted strong airglow lines do not affect the solution due to masking the narrow 15 \AA -wide regions around them. The resulted stellar parameters are LOS velocity v , velocity dispersion σ , higher order Gauss–Hermite coefficient h_3, h_4 and the stellar population parameters: the age T and metallicity $[Z/H]$. The radial profiles of the parameters for SCORPIO data are partly shown in Katkov et al. (2014a), also will be appeared in Katkov et al. (2014b); the paper with SALT data results is in preparation (Katkov et al. in preparation).

For the full spectral fitting we utilized solar alpha-enhanced stellar population models which doesn't provide properties of alpha-enrichments of stellar population. In order to estimate $[Mg/Fe]$ also we measured Lick indices and estimated $[Mg/Fe]$ by comparison with the evolutionary SSP models by (Thomas et al. 2003).

4. Stellar populations

In order to compare stellar population properties of different galactic components (bulges, discs, lens/ring) we have averaged radial profiles in the region where each component have dominant contribution. We computed azimuthally averaged surface brightness profiles using photometric data from SDSS (DR9), 2MASS and direct imaging in 6-m telescope and determined the dominance regions for every structural component of galaxy. We marked out disc regions where surface brightness profiles are exactly fitted by exponential profile. The averaged stellar parameters are shown in Table 1, Figures 1, 3, 2 and 5 represent stellar population properties and comparison between them for different galactic components.

4.1. Comparison of stellar populations for bulge, disc, lens/ring.

The next step is a comparison of stellar population properties of various components of galaxies. The ratio of average ages produces a sequence of major evolutionary stages in the galactic evolution path, and the α -element abundance ratio $[Mg/Fe]$ limits the epoch of star formation.

4.1.1. Bulges vs. discs

In the standard Λ CDM cosmology (Blumenthal et al. 1984) galaxies assemble through hierarchical merging and then evolve under a combination of internal and environmental processes. In this paradigm the classical bulges are formed firstly by major merging and then the large-scale disc components are assembled by smoothed cold gas accretion (Governato et al. 2004, 2007). However, there are observational evidences

However, there are observational evidences contradicting these predictions: the studies of the surface photometry of galaxies consistently demonstrate the correlation between the characteristic scales of bulges and discs, and the presence of this correlation does not depend on the type of bulges – classical bulge or pseudo-bulges (MacArthur et al. 2003; Méndez-Abreu et al. 2008; Laurikainen et al. 2010). Thus, the formation of bulge and disc structure of galaxy seems to be synchronized in galaxies.

It is supported by Fig. 3 (*upper left*). At first sight the dependence of age of discs against bulges looks rather “smeared”, however the correlation coefficient (Pearson) is equal 0.66. At Fig. 3 (*upper left*) the green dotted lines denote the area where measurements deviate from bisector less then 0.2 dex (in 1.5 times), blue dotted lines – less then 0.3 dex (in 3 times). The ± 0.2 dex region consist of 63% (10/16) measurements, the ± 0.2 dex region – 75% (12/16). So, the comparison of stellar ages of bulges and discs shows a tendency to equal ages of bulge and disc component.

The ages measurements of the isolated lenticular galaxies essentially differ from measurements for galaxies in the dense environment: the points are grouped in the left top corner, over a bisector – the ages of discs are equal, or older in comparison with the bulge ages (Sil'chenko et al. 2012). That difference between group/cluster galaxies and galaxies in sparse environment is expected. Because all physical mechanisms of external impact related to dense environment, both gravitational and gas-dynamic, lead to gas flows down to the galaxy center and provoke the subsequent star formation bursts in the center and bulge rejuvenation (Bekki & Couch 2011; Kronberger et al. 2008).

It is interesting that the alpha abundance ratio is identical for bulges and discs (see. Fig. 3, *right*). We calculated a linear fit ($[Mg/Fe]_{disc} = a + b[Mg/Fe]_{bulge}$) taking into account error bars along both axes and found no significant deviations of zero-point from zero level as well

Galaxy	N	T, Gyr	[Z/H], dex	[Mg/Fe], dex,	σ , km/s
Bulge					
IC 1502	11	17.7 \pm 1.0	-0.04 \pm 0.06	0.32 \pm 0.10	165 \pm 12
IC 1608	3	4.6 \pm 0.2	-0.24 \pm 0.05	0.12 \pm 0.09	147 \pm 5
IC 3152	6	5.1 \pm 0.3	-0.28 \pm 0.07	0.12 \pm 0.09	186 \pm 12
NGC 16	10	5.4 \pm 0.8	-0.04 \pm 0.05	0.19 \pm 0.04	172 \pm 6
NGC 1211	4	2.5 \pm 1.0	-0.16 \pm 0.07	0.11 \pm 0.07	163 \pm 16
NGC 2350	8	1.5 \pm 0.4	-0.13 \pm 0.10	–	107 \pm 12
NGC 2917	4	5.9 \pm 1.2	-0.20 \pm 0.06	0.27 \pm 0.08	192 \pm 9
NGC 3098	10	5.4 \pm 0.3	-0.10 \pm 0.02	0.00 \pm 0.02	74 \pm 6
NGC 3248	10	4.8 \pm 0.6	-0.11 \pm 0.05	0.00 \pm 0.05	77 \pm 5
NGC 4240	6	4.6 \pm 0.5	-0.32 \pm 0.10	0.18 \pm 0.09	109 \pm 3
NGC 6010	3	8.3 \pm 0.4	-0.23 \pm 0.04	0.19 \pm 0.06	152 \pm 5
NGC 6615	8	10.8 \pm 1.6	-0.26 \pm 0.05	0.24 \pm 0.03	129 \pm 5
NGC 6654	9	12.2 \pm 1.4	-0.19 \pm 0.07	0.23 \pm 0.04	158 \pm 5
NGC 6798	8	8.3 \pm 0.9	-0.20 \pm 0.07	0.13 \pm 0.04	115 \pm 7
NGC 7351	8	2.0 \pm 0.1	-0.27 \pm 0.03	-0.03 \pm 0.06	53 \pm 6
UGC 4551	8	9.9 \pm 1.8	-0.28 \pm 0.08	0.15 \pm 0.03	158 \pm 10
UGC 9519	8	2.4 \pm 0.2	-0.11 \pm 0.07	0.04 \pm 0.03	76 \pm 3
UGC 9980	4	7.7 \pm 0.3	-0.27 \pm 0.04	0.18 \pm 0.11	142 \pm 6
Disc					
IC 1502	11	16.7 \pm 1.7	-0.13 \pm 0.10	0.42 \pm 0.01	130 \pm 25
IC 1608	8	3.2 \pm 0.7	-0.43 \pm 0.14	0.18 \pm 0.15	141 \pm 16
IC 3152	8	3.6 \pm 2.3	-1.19 \pm 0.42	0.20 \pm 0.13	161 \pm 28
NGC 16	18	1.6 \pm 1.2	-0.19 \pm 0.16	0.16 \pm 0.02	127 \pm 18
NGC 1211	2	10.0 \pm 2.5	-1.48 \pm 0.13	–	145 \pm 58
NGC 2350	14	1.2 \pm 0.2	-0.00 \pm 0.07	0.06 \pm 0.07	89 \pm 14
NGC 2917	0	–	–	–	–
NGC 3098	19	5.2 \pm 1.5	-0.22 \pm 0.06	0.08 \pm 0.02	56 \pm 26
NGC 3248	31	3.9 \pm 1.4	-0.21 \pm 0.09	-0.04 \pm 0.03	65 \pm 17
NGC 4240	5	4.8 \pm 1.6	-1.03 \pm 0.11	0.33 \pm 0.13	112 \pm 30
NGC 6010	11	4.6 \pm 1.4	-0.34 \pm 0.16	0.18 \pm 0.04	115 \pm 13
NGC 6615	0	–	–	–	–
NGC 6654	3	5.8 \pm 0.6	-0.06 \pm 0.14	0.40 \pm 0.20	44 \pm 5
NGC 6798	22	3.4 \pm 2.4	-0.30 \pm 0.21	0.11 \pm 0.12	122 \pm 20
NGC 7351	7	5.4 \pm 3.5	-0.62 \pm 0.20	-0.02 \pm 0.15	80 \pm 33
UGC 4551	1	12.0 \pm 0.0	-0.61 \pm 0.00	0.25 \pm 0.25	103 \pm 0
UGC 9519	4	3.0 \pm 1.4	-0.38 \pm 0.12	0.15 \pm 0.20	94 \pm 14
UGC 9980	6	9.7 \pm 3.0	-0.97 \pm 0.10	0.21 \pm 0.20	100 \pm 33
Lens/Ring					
IC 1502	0	–	–	–	–
IC 1608	10	3.2 \pm 1.7	-0.79 \pm 0.20	0.24 \pm 0.08	100 \pm 17
IC 3152	0	–	–	–	–
NGC 16	16	3.3 \pm 2.9	-0.25 \pm 0.16	–	104 \pm 16
NGC 1211	12	4.9 \pm 1.8	-0.79 \pm 0.24	0.20 \pm 0.18	152 \pm 17
NGC 2350	1	4.9 \pm 0.0	-0.33 \pm 0.00	–	97 \pm 0
NGC 2917	10	2.5 \pm 0.3	-0.34 \pm 0.07	0.24 \pm 0.07	131 \pm 14
NGC 3098	13	4.7 \pm 1.2	-0.12 \pm 0.04	0.05 \pm 0.01	58 \pm 12
NGC 3248	0	–	–	–	–
NGC 4240	0	–	–	–	–
NGC 6010	0	–	–	–	–
NGC 6615	3	12.8 \pm 2.4	-0.52 \pm 0.16	0.21 \pm 0.06	56 \pm 5
NGC 6654	0	–	–	–	–
NGC 6798	20	1.9 \pm 1.5	-0.33 \pm 0.17	0.13 \pm 0.04	96 \pm 20
NGC 7351	0	–	–	–	–
UGC 4551	11	3.2 \pm 2.1	-0.44 \pm 0.17	0.23 \pm 0.03	118 \pm 24
UGC 9519	23	2.6 \pm 0.5	-0.22 \pm 0.07	0.05 \pm 0.02	78 \pm 9
UGC 9980	6	5.1 \pm 1.4	-0.37 \pm 0.09	–	126 \pm 9

Table 1: Averaged stellar population parameters

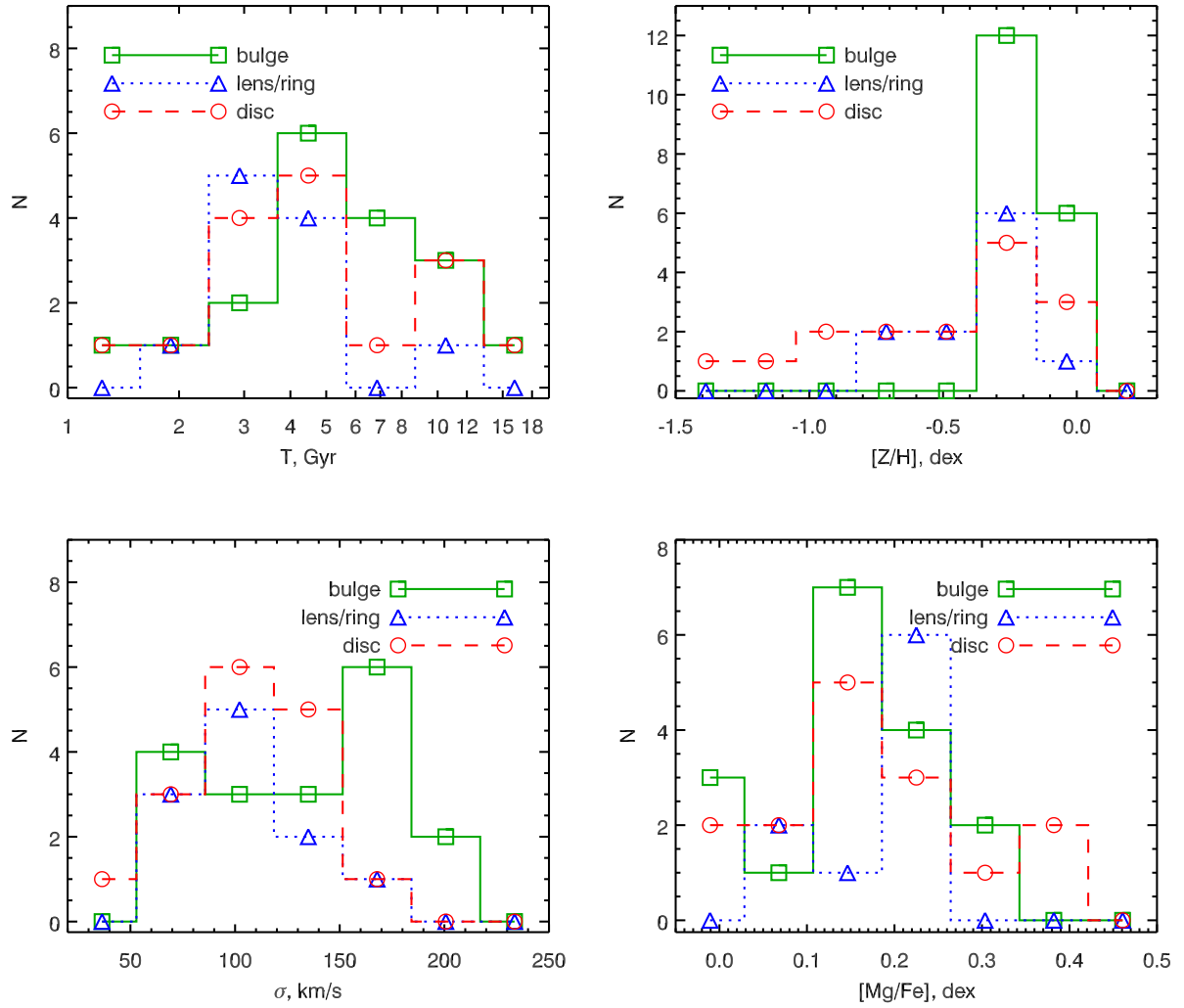


Fig. 1.— Histogram for ages metallicities, velocity dispersion and $[Mg/Fe]$ for different stellar substructures of galaxies.

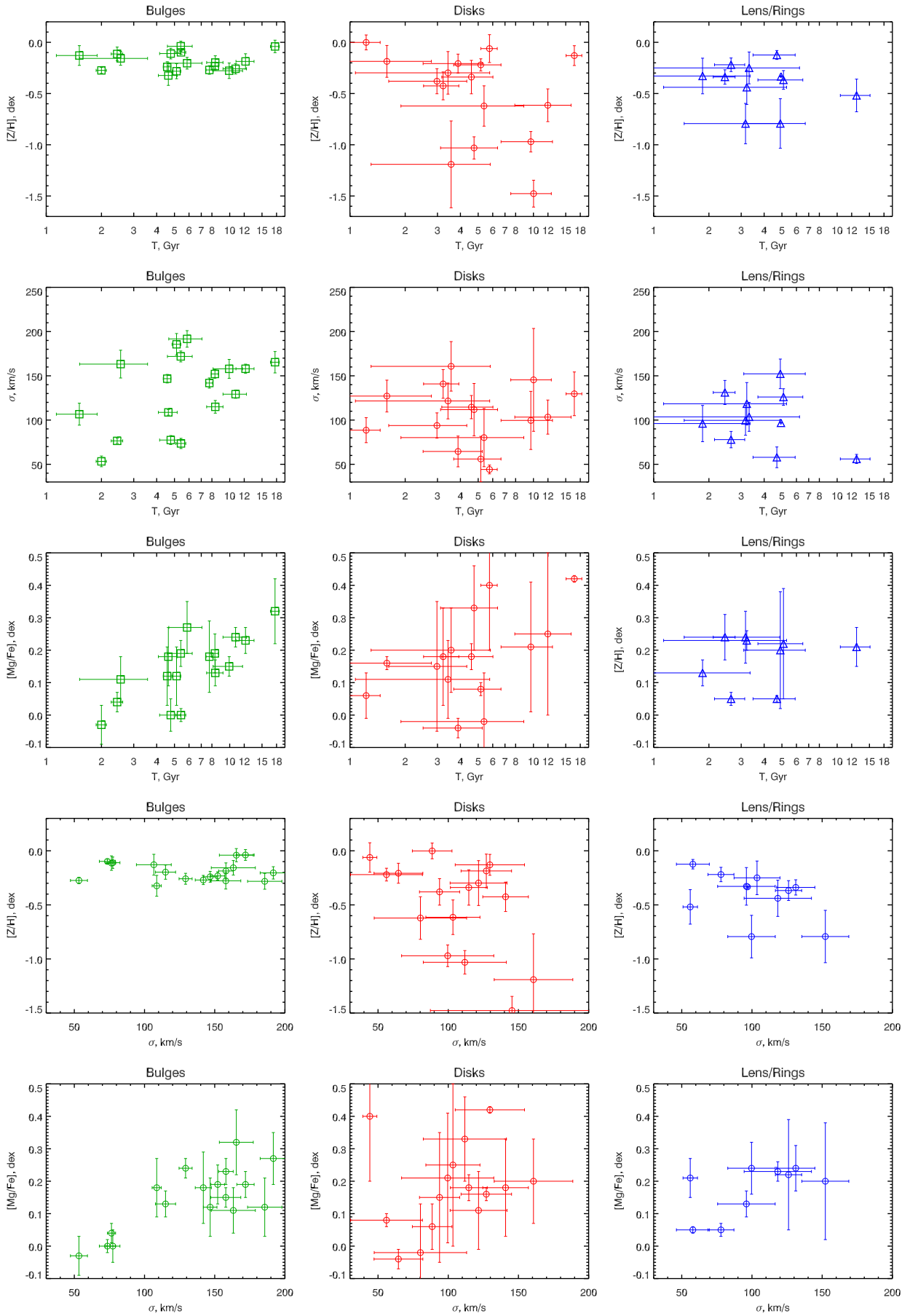


Fig. 2.— Parameter dependancies for bulges, disc and lens/ring.

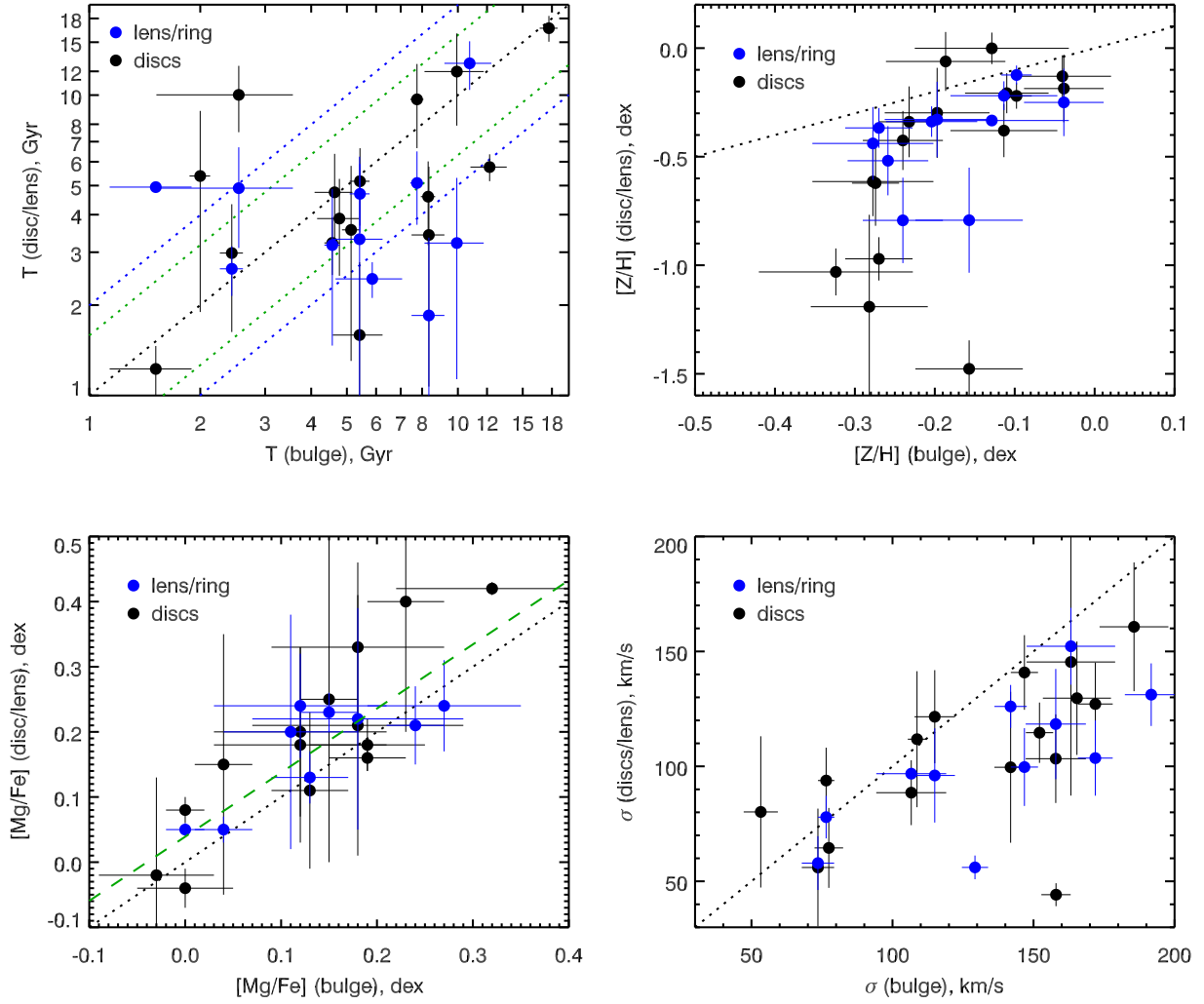


Fig. 3.— Comparison of stellar population properties between bulges and disc, lens/ring. Dotted line corresponds to equilibrium line. Green dashed line shows a linear fit taking into account error bars along X as well as Y direction.

as slope of dependence: $a = 0.04 \pm 0.05$, $b = 0.9 \pm 0.3$. The strong correlation ($R_P = 0.88$) implies that the star formation fades quickly or continues during billions years simultaneously both in bulges and discs. This result allows us to strengthen the thesis about synchronous formation of bulges and discs: the star formation starts and stops quasi-simultaneously in both components. The stellar metallicity of discs is lower than bulges. That possibly means that the low-metallicity gas accretes generally onto the disc where gas is enriched by metals and goes down to the bulge region.

Based on Kormendy diagram (dependence of V/σ ratio on isophotal ellipticity, Fig. 4) and relationship between bulge and disc velocity dispersion it appeared equally pseudo-bulges and dynamically heated classical bulges. It confirms once again that bulges in the lenticular galaxies are very various on luminosity and a contribution to the total galaxy mass as well as by origin and evolution. It is true also if we consider the *isolated* S0 galaxies, for which the impact of an environment on evolution seems to be minimized.

4.1.2. Disc substructures: lenses and rings

The lenses in S0 galaxies are considered genetically connected with starforming rings in past. Still the prevailed point of view that stellar population in lenses are old, and dynamically they are hot (Kormendy 1984; Laurikainen et al. 2013). However, this opinion is based on studying of a single objects. We were able to determine stellar population properties in 10 lenses/rings in our galaxies. On average, the lenses/rings show the same velocity dispersion as the discs (Fig. 5 *right bottom*). Except NGC 6615 ($T_{lens} = 13$ Gyr), all measurements in the lenses/rings are not so old, but have intermediate ages in the narrow range 2 – 5 Gyr ($z = 0.3 - 0.5$), thus discs ages cover significantly wider range. It means that the rings formation epoch isn't connected with formation of discs. On average, the chemical abundances ($[Z/H]$, $[Mg/Fe]$) in the lenses and rings are the same as in discs, except only NGC 1211 where disc is extremely metal-poor.

4.2. Epoch and duration of formation stellar content

The comparison between the alpha element abundance ratio $[Mg/Fe]$, characterized duration of last star formation burst, and other stellar population properties for galaxy components are shown at Fig. 6. And again we see synchronism of bulge evolution and discs. The correlation of the relation of $[Mg/Fe]$ with velocity dispersion of the stars, characterizing the local density of gravitating mass, is known long ago for elliptical galaxies and for bulges Trager et al. (2000); it is considered as the evidence for relationship of star formation efficiency and depth of potential well. However, Fig. 6 (*left*) and Fig. 2 (*bottom row*), for the first time we see that this correlation is not only for bulges, but also for discs. By analogy

it is possible to assume that the accretion rates of external gas are higher when the local potential well in the plane of disc is deeper, and higher rate of accretion provides more effective star formation.

At Fig. 6 (*center*) we compare element ratios Mg/Fe with stellar ages. We plot dotted envelop line; the points concentrate near this line or on the left of this line. Probably it is due to the fact that galaxies (and subcomponents) which have begun the formation at the same time in the early Universe, on $z = 2 - 3$, have stopped it in different way. Galaxies, which finished star formation quickly, reveal average older age and higher $[Mg/Fe]$ abundance ratio; galaxies, where star formation continues during many Gyr's, decrease their $[Mg/Fe]$ abundance ratio down to solar value. At Fig. 6 (*center*) there are cloud of points on left of dotted line consisted of bulge and disc measurements. These are stellar systems in which the last event of a star formation took place *later*, than at the main population of galaxies. Indeed, in order to have ages of 1.5 – 3 Gyr and $[Mg/Fe]=+0.2$, the galaxy needs to experience 1.0 – 1.5 billion years of an active star formation significantly later than $z = 0.5$. Thus, it turns out that star formation events in the isolated lenticular galaxies can happen at different times and have different duration.

4.3. Formation scenario

The results presented in this section confirmed the strong influence environment on evolution and stellar population properties of galaxies: there is no allocated epoch of formation of structural components, they can grow their stellar population on $z > 2$ as well as only billion years ago. Our findings support the idea that the dispersion of average ages in discs of S0 galaxies increases with decrease with environment density of galaxies (Sil'chenko et al. 2012) and reaches a maximum among the isolated galaxies.

On what the morphological type of disc galaxy in sparse environment depends? Why it can be lenticular or spiral galaxy at current epoch? Everything agrees on a mode of external cold gas accretion which usually feeds a star formation in discs of spiral galaxies throughout many billions years. The gas accretion happens quite possibly by stochastic mode.

Recent work by Karachentseva et al. (2011) on search of dwarf satellites near isolated galaxies reveals curious statistical feature. The radial velocity difference between satellites and host galaxy is higher for lenticular galaxies than for spirals, moreover lenticular galaxies have no satellites with velocity difference $< 50 \text{ km s}^{-1}$. Probably this dynamic feature indicates that the satellites of lenticular galaxies can't fall onto the host galaxy, whereas it is quite enough dynamic friction in order to provide satellite accretion onto spirals. In other words, orbital configurations of dwarf satellites of a galaxy are formed in a stochastic way. Disk galaxies possessing dynamically cold system of satellites will provide themselves by gas

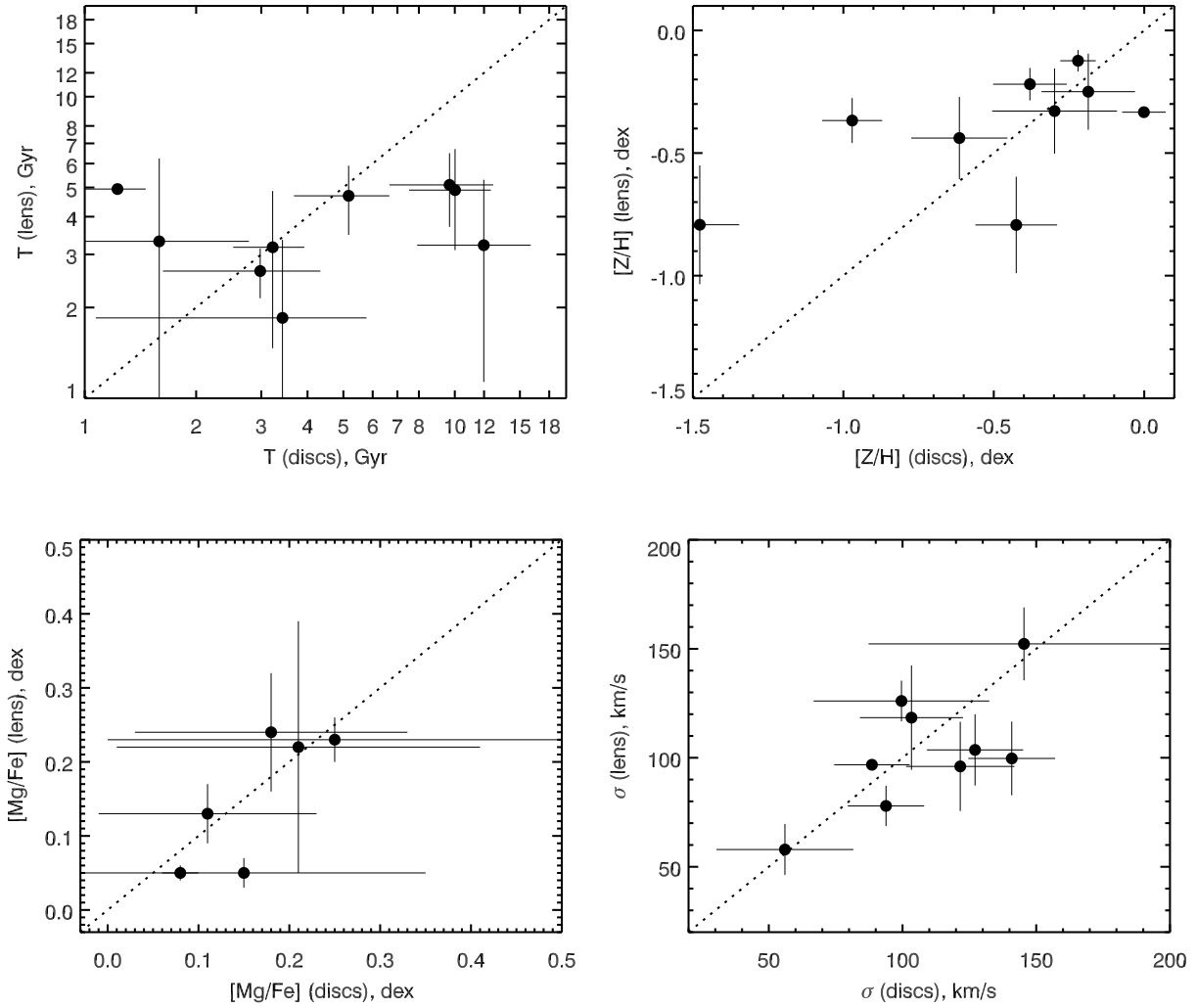


Fig. 5.— Comparison of stellar population properties between discs and lenses/rings.

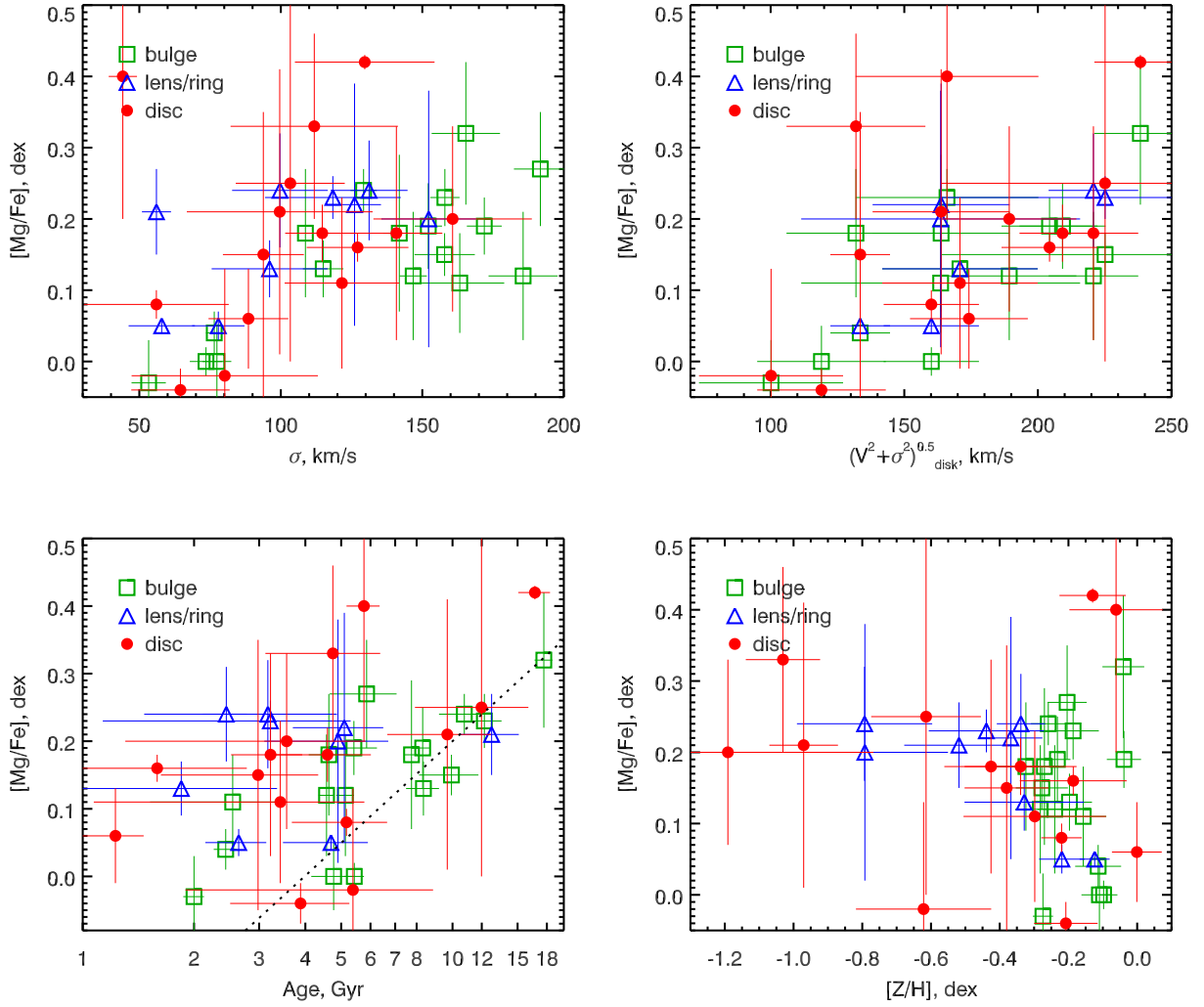


Fig. 6.— The alpha-abundance ($[Mg/Fe]$) against velocity dispersion, dynamical parameter $(V^2 + \sigma^2)^{0.5}$, ages and metallicity for bulges, discs, lenses/rings.

“fuel” for star formation and subsequent transformation into spiral galaxy. The main physical processes for transformation are minor merging and tidal accretion. If the galaxy can’t provide itself by “fuel” for star formation due to dynamical hot state of satellite system or due to absence of dwarf which can be fall onto the galaxy, then the galaxy will become lenticular.

5. Ionized gas

We found large-scale ionized gas structures in most objects of our sample of galaxies. For such objects we obtained pure emission-line spectrum by subtracting the stellar contribution (i.e., the best-fitting stellar population model) from the observed spectrum. This step provided a pure emission spectrum uncontaminated by absorption lines of the stellar component that is especially important for the Balmer lines. Then we fitted emission lines with Gaussians pre-convolved with the instrumental LSF in order to determine the LOS velocities of the ionized gas and emission-line fluxes.

The line fluxes have been corrected for the internal interstellar extinction as well as for the Galactic extinction according to Schlegel et al. (1998). The color excess $E(B - V)$ corresponding to the internal dust reddening was determined from the Balmer decrement using the theoretical line ratios $F(\text{H}\alpha)/F(\text{H}\beta) = 2.87$ for the electron temperature $T_e = 10,000$ K (Osterbrock & Ferland 2006) and the parameterized extinction curve (Fitzpatrick 1999). We plotted our measurements of emission lines onto the classical excitation-type BPT (Baldwin, Phillips & Terlevich) diagnostic diagrams Baldwin et al. (1981) to identify the gas ionization source.

The results and discussion for the SCORPIO part of our sample are presented in Katkov et al. (2014a, 2013). Here we repeat conclusions based on full SCORPIO+SALT sample of galaxies.

5.1. Statistics of ionized gas decouplings

Based on analysis of long-slit spectroscopic data obtained at 6-m BTA telescope as well as at SALT telescope, we found that 13 out of 18 ($72 \pm 11\%$) observed lenticular galaxies reveal extended emission lines; and among those, 6 galaxies ($46 \pm 14\%$) demonstrate decoupled gas kinematics respect to their stellar discs.

By comparing our results on the frequency of extended ionized gas discs in S0 galaxies with the earlier statistics, we see full agreement: Kuijken et al. (1996) found ionized gas in 17 of 29 S0s studied, so their fraction of gas-rich S0s is about $58 \pm 9\%$ per cent, just as in our study. However, if we consider a fraction of counterrotating gaseous discs among all extended gaseous discs in S0 galaxies, we see a prominent difference. When S0 galaxies were selected over all types of environment, the fraction of counterrotating gaseous discs was 20 – 24 per cent ((Bertola et al. 1992; Kuijken et al. 1996)); more exactly, by combining two samples, Kuijken et al. (1996) gave 24 ± 8 per cent. In our sample, the fraction of coun-

terrotating gaseous discs is higher, 46 ± 14 per cent. We expected such a trend because Davis et al. (2011) noted a dependence of gas kinematics in the early-type galaxies (mostly S0s in the ATLAS-3D sample) on their environment: dense environment provided tight coincidence between gas and star kinematics while in more sparse environments the fraction of decoupled gaseous kinematics grew. Our isolated S0 galaxies represent an extreme point in this dependency.

Following the logic of Bertola et al. (1992) according to which when gas is accreted, it should have an arbitrary spin, and so long-slit spectroscopy should reveal an equal fraction of corotating and counterrotating gaseous discs. If one takes into account the possibility for internal gas incidence, the fraction of systems with counterrotating gaseous discs would be less than 50 per cent. But our results based on the full SCORPIO+SALT sample of galaxies in the strictly sparse environment suggest that the fraction of the gas counterrotations is 50 per cent. Hence, we can conclude that in isolated S0s their gas is virtually always accreted from external sources. But to be certain that the directions of possible gas accretion are distributed isotropically, we must first identify sources of gas accretion. Our galaxies are isolated so they cannot acquire their gas from neighbours of comparable mass/luminosity; the sources of cold gas accretion may be dwarf satellite merging (Kaviraj et al. 2009, 2011) or perhaps cosmological gas filaments (Dekel & Birnboim 2006; Kereš et al. 2005). Are they distributed isotropically? This is an open question.

5.2. Metallicity and origin of gas structures

Based on diagnostic BPT diagrams we marked out a regions where photoionization by young stars is a dominant excitation mechanism. We binned pure emission spectra in such regions in order to increase signal-to-noise ratio and determined emission line fluxes. We estimated oxygen abundances by utilizing $O2N2$ and $N2$ calibrations proposed by Pettini & Pagel (2004). The $N2$ calibration was used for bins where signal-to-noise ratios for $\text{H}\beta$ and $[\text{O III}]$ were poor, $S/N < 3$. The oxygen abundances as well as the radii for binned regions are shown at Table 2.

There is a large diversity of galaxy gas/star subsystems which have orbital momentum distinguishing compared to stellar disc: inner polar rings/discs, large-scale outer polar rings/disc, counter-rotating stellar/gaseous discs, polar bulges and inner nuclear discs. Based on dynamic considerations no doubt that these structures are formed from an external material acquired during gravitational interactions with other galaxies or by external accretion processes, which can occur throughout the life of the galaxy. The properties and morphological appearance of resulted decoupled subsystems depend on geometry, angular momentum of accreted material and duration of accretion.

Several acquisition scenario of the external gas are

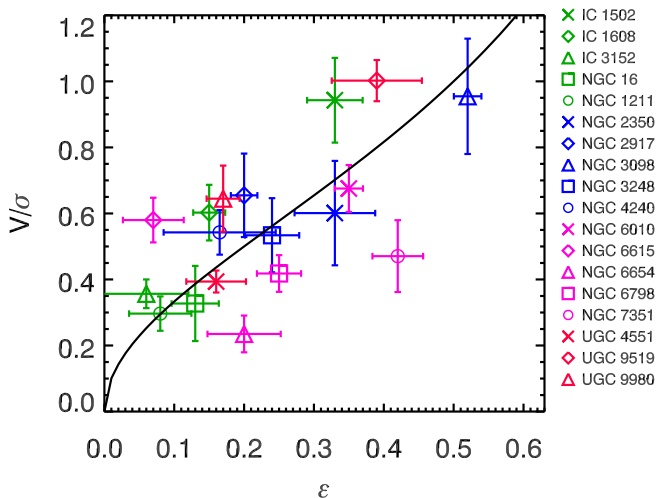


Fig. 4.— Kormendy diagram: ratio between velocity rotation and stellar velocity dispersion V/σ against isophote ellipticity ϵ . Solid line correspond to isotropic rotationally supported spheroids.

Galaxy	Binning region	$12+\log O/H ([Z/H]_{\odot})$ dex
IC 1608	(-51.4; -31.1) (29.7; 43.4)	8.78 (0.09) \pm 0.47 8.80 (0.11) \pm 0.26
IC 3152 ^{N2}	(-12.6; -8.1) (4.1; 10.2)	8.73 (0.04) \pm 0.42 8.78 (0.09) \pm 0.42
IC 4653	(-5.6; 4.6)	8.57 (-0.12) \pm 0.25
NGC 1211 ^{N2}	(9.4; 15.8) (32.3; 37.3)	8.72 (0.03) \pm 0.41 8.73 (0.04) \pm 0.41
NGC 2917	(-15.7; -5.6) (9.6; 19.8)	8.90 (0.21) \pm 0.27 8.82 (0.13) \pm 0.26
NGC 4240 ^{N2}	(-11.6; -6.6) (4.1; 12.2)	8.80 (0.11) \pm 0.41 8.78 (0.09) \pm 0.41
NGC 9980 ^{N2}	(-13.1; -4.3) (8.4; 20.8)	8.82 (0.13) \pm 0.42 8.71 (0.02) \pm 0.42
NGC 2350	(-1.6; 2.0)	8.68 (-0.01) \pm 0.25
NGC 6798 ^{N2}	(-34.1; -27.7) (29.1; 36.6)	8.71 (0.02) \pm 0.41 8.73 (0.04) \pm 0.41
NGC 7351	(-2.7; 3.8)	8.64 (-0.05) \pm 0.25

Table 2: Oxygen abundances in star forming regions.

considered in the literature:

1. The major dissipative merger. The acquisition of the gas results from a merger of two disc galaxies with unequal mass with orbits close to “polar” (Bekki 1998; Bournaud et al. 2005).
2. Tidal accretion. Decoupled gas structures may form by the disruption of a dwarf companion galaxy orbitating around an early-type system or by gas stripping from disc galaxy outskirts, captured by galaxy on a parabolic encounter (Reshetnikov & Sotnikova 1997; Bournaud & Combes 2003).
3. Cold gas accretion from cosmological filaments. Recent theoretical works Kereš et al. (2005); Dekel & Birnboim (2006); Bournaud & Elmegreen (2009) which are based on numerical simulation, emphasize the important role of cold gas accretion for the formation of disc galaxies. It was shown in context of cosmological simulation, that the cold gas accretion from several filament which are in the different planes, will lead to formation of kinematically decoupled substructures (Dekel et al. 2009; Roškar et al. 2010; Algorry et al. 2014). The acquired gas from filament has to possess extremely low metallicity, and taking into account possible mixture of pristine gas with enriched gas stripped from satellites, metallicity shouldn’t exceed 1/10 solar value (Agertz et al. 2009).

The scenario of major mergers is excluded because the isolated lenticular galaxies has no massive “neighbors” by definition. The tidal accretion scenario can be considered in the case of interaction with dwarf satellites, excepting tidal gas accretion from outskirts of giant galaxies. The key parameter by means of which it is possible to make a choice between tidal accretion and cold gas accretion from filaments is metallicity of gas. Our measurements of oxygen abundance of ionized gas in the star forming region in isolated S0 galaxies indicates a solar metallicity (see Table 2) that excludes accretion from filaments.

5.3. Luminosity-metallicity relation

The correlation between luminosity or mass of galaxies with the metals enrichment of gas is the well-known observation fact. For the first time this correlation were found for irregular and blue compact galaxies (Lequeux et al. 1979; Kinman & Davidson 1981), soon after and for disc galaxies (Rubin et al. 1984). The subsequent studies of nearby galaxies only strengthened conclusions about mass/luminosity-metallicity relation (see for ex. Tremonti et al. (2004) and references therein). Various physical mechanisms are proposed for the explanation of mass-metallicity relation: 1) the loss of enriched gas by outflow caused by SN explosions (Tremonti et al. 2004; Kobayashi et al. 2007); 2) the accretion of pristine gas by inflows from intergalactic medium Finlator & Davé (2008); 3) variations of the initialmass function with

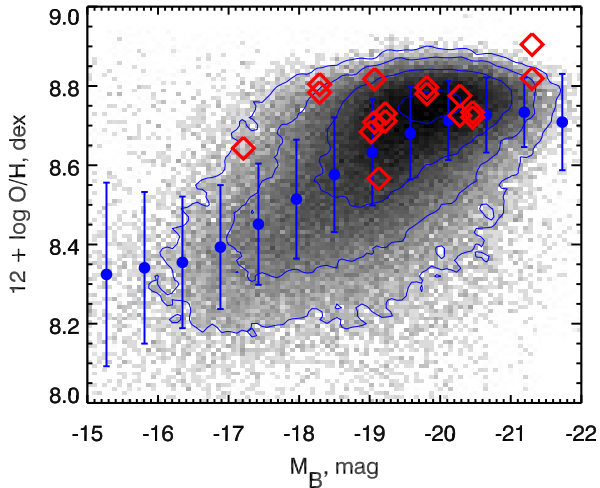


Fig. 7.— Dependence gas metallicity on absolute B magnitude. Grey distribution correspond to SDSS data. Blue points shows median values if distribution in bins by magnitude value. Red points shows our measurements in isolated lenticular galaxies.

galaxy mass Köppen et al. (2007); 4) sformation efficiencies in low-mass galaxies caused by supernova feedback (downsizing) Brooks et al. (2007) or a combination of them.

At Fig. 7 we plotted luminosity-metallicity for SDSS data and overlapped our measurements of metallicities in star forming regions in isolated S0 galaxies. Despite the wide range of luminosities there is no strong correlation between our measurements of oxygen abundances with absolute B magnitudes. Most of our measurements doesn't match averaged distribution of luminosity-metallicity distribution (blue points). Probably it indicates that chemical evolution of ionized gas in isolated lenticulars doesn't relate to individual properties of galaxies, what coincides and strengthens a conclusion about an external origin of gas. In the context of scenario of tidal gas accretion from the dwarf satellites, the narrow range of metallicity estimates in our galaxies makes a hint about homogeneous properties of satellites.

6. Conclusions

In this work we have presented the results of deep long-slit spectroscopy (total exposures per target 0.3-3 hour) with the 6-m Russian telescope and with Southern African Large Telescope (SALT) for sample of 18 isolated lenticular galaxies. By using full spectral fitting technique as well as Lick indices approach and by analysing of the pure emission line spectra we have obtain that:

- The obtained average ages of the stellar populations in bulges and discs covers a wide range between 1.5 and > 15 Gyr, that indicates the absence of distinct epoch of their stellar content formation.

- In contrast to galaxies in groups and clusters, the stellar population ages in bulges and discs of isolated lenticulars tend to be equal, that supports the inefficiency of the bulge rejuvenation in sparse environment.
- Almost all the lenses and rings possess intermediate ages of the stellar populations, within the range of 2 – 5 Gyr. On average, the chemical abundances ($[Z/H]$, $[Mg/Fe]$) in the lenses and rings are the same as in discs, also dynamically the stellar population in lenses and rings do not sufficiently stand out against a discs.
- More than half of the sample of isolated lenticulars (72 ± 11 %) possess extended emission-line structures; among those, 6 galaxies (46 ± 14 %) demonstrate decoupled gas kinematics with respect to their stellar discs.
- We have found starforming off-nuclear regions in 10 galaxies; their gas oxygen abundances are nearly solar that implies tidal gas accretion from gas-rich dwarf satellites rather than accretion from cosmological large-scale structure filaments.

REFERENCES

- Afanasiev, V. L., & Moiseev, A. V. 2011, *Baltic Astronomy*, 20, 363
- Agertz, O., Teyssier, R., & Moore, B. 2009, *Monthly Notices Roy. Astron. Soc.*, 397, L64
- Algorry, D. G., Navarro, J. F., Abadi, M. G., et al. 2014, *Monthly Notices Roy. Astron. Soc.*, 437, 3596
- Baldwin, J. A., Phillips, M. M., & Terlevich, R. 1981, *PASP*, 93, 5
- Bekki, K. 1998, *Astrophys. J.*, 499, 635
- Bekki, K., & Couch, W. J. 2011, *Monthly Notices Roy. Astron. Soc.*, 415, 1783
- Bertola, F., Buson, L. M., & Zeilinger, W. W. 1992, *Astrophys. J. Let.*, 401, L79
- Blumenthal, G. R., Faber, S. M., Primack, J. R., & Rees, M. J. 1984, *Nature*, 311, 517
- Bournaud, F., & Combes, F. 2003, *Astron. and Astrophys.*, 401, 817
- Bournaud, F., & Elmegreen, B. G. 2009, *Astrophys. J. Let.*, 694, L158
- Bournaud, F., Jog, C. J., & Combes, F. 2005, *Astron. and Astrophys.*, 437, 69
- Brooks, A. M., Governato, F., Booth, C. M., et al. 2007, *Astrophys. J. Let.*, 655, L17
- Burgh, E. B., Nordsieck, K. H., Kobulnicky, H. A., et al. 2003, in *Society of Photo-Optical Instrumentation Engineers (SPIE) Conference Series*, Vol. 4841, Instrument Design and Performance for Optical/Infrared Ground-based Telescopes, ed. M. Iye & A. F. M. Moorwood, 1463–1471
- Byrd, G., & Valtonen, M. 1990, *Astrophys. J.*, 350, 89
- Chilingarian, I., Prugniel, P., Sil'Chenko, O., & Koleva, M. 2007a, in *IAU Symposium*, Vol. 241, IAU Symposium, ed. A. Vazdekis & R. Peletier, 175–176
- Chilingarian, I. V., Prugniel, P., Sil'Chenko, O. K., & Afanasiev, V. L. 2007b, *Monthly Notices Roy. Astron. Soc.*, 376, 1033

- Crawford, S. M., Still, M., Schellart, P., et al. 2010, in Society of Photo-Optical Instrumentation Engineers (SPIE) Conference Series, Vol. 7737, Society of Photo-Optical Instrumentation Engineers (SPIE) Conference Series
- Davis, T. A., Alatalo, K., Sarzi, M., et al. 2011, *Monthly Notices Roy. Astron. Soc.*, 417, 882
- Dekel, A., & Birnboim, Y. 2006, *Monthly Notices Roy. Astron. Soc.*, 368, 2
- Dekel, A., Birnboim, Y., Engel, G., et al. 2009, *Nature*, 457, 451
- Finlator, K., & Davé, R. 2008, *Monthly Notices Roy. Astron. Soc.*, 385, 2181
- Fitzpatrick, E. L. 1999, *PASP*, 111, 63
- Governato, F., Willman, B., Mayer, L., et al. 2007, *Monthly Notices Roy. Astron. Soc.*, 374, 1479
- Governato, F., Mayer, L., Wadsley, J., et al. 2004, *Astrophys. J.*, 607, 688
- Gunn, J. E., & Gott, III, J. R. 1972, *Astrophys. J.*, 176, 1
- Icke, V. 1985, *Astron. and Astrophys.*, 144, 115
- Karachentsev, I. D., & Makarov, D. I. 2008, *Astrophysical Bulletin*, 63, 299
- Karachentsev, I. D., Makarov, D. I., Karachentseva, V. E., & Melnyk, O. V. 2011, *Astrophysical Bulletin*, 66, 1
- Karachentseva, V. E., Karachentsev, I. D., & Melnyk, O. V. 2011, *Astrophysical Bulletin*, 66, 389
- Katkov, I., Sil'chenko, O., & Afanasiev, V. 2013, ArXiv e-prints, arXiv:1312.6572
- Katkov, I. Y., & Chilingarian, I. V. 2011, in *Astronomical Society of the Pacific Conference Series*, Vol. 442, *Astronomical Data Analysis Software and Systems XX*, ed. I. N. Evans, A. Accomazzi, D. J. Mink, & A. H. Rots, 143
- Katkov, I. Y., Kniazev, A. Y., & Sil'chenko, O. K. in preparation
- Katkov, I. Y., Moiseev, A. V., & Sil'chenko, O. K. 2011, *Astrophys. J.*, 740, 83
- Katkov, I. Y., Sil'chenko, O. K., & Afanasiev, V. L. 2014a, *Monthly Notices Roy. Astron. Soc.*, 438, 2798
- . 2014b, *Astrophysical Bulletin*, 60, 121
- Kaviraj, S., Peirani, S., Khochfar, S., Silk, J., & Kay, S. 2009, *Monthly Notices Roy. Astron. Soc.*, 394, 1713
- Kaviraj, S., Tan, K.-M., Ellis, R. S., & Silk, J. 2011, *Monthly Notices Roy. Astron. Soc.*, 411, 2148
- Kereš, D., Katz, N., Weinberg, D. H., & Davé, R. 2005, *Monthly Notices Roy. Astron. Soc.*, 363, 2
- Kinman, T. D., & Davidson, K. 1981, *Astrophys. J.*, 243, 127
- Kniazev, A. Y., Zijlstra, A. A., Grebel, E. K., et al. 2008, *Monthly Notices Roy. Astron. Soc.*, 388, 1667
- Kobayashi, C., Springel, V., & White, S. D. M. 2007, *Monthly Notices Roy. Astron. Soc.*, 376, 1465
- Kobulnicky, H. A., Nordsieck, K. H., Burgh, E. B., et al. 2003, in *Society of Photo-Optical Instrumentation Engineers (SPIE) Conference Series*, Vol. 4841, *Instrument Design and Performance for Optical/Infrared Ground-based Telescopes*, ed. M. Iye & A. F. M. Moorwood, 1634–1644
- Köppen, J., Weidner, C., & Kroupa, P. 2007, *Monthly Notices Roy. Astron. Soc.*, 375, 673
- Kormendy, J. 1984, *Astrophys. J.*, 286, 116
- Kronberger, T., Kapferer, W., Ferrari, C., Unterguggenberger, S., & Schindler, S. 2008, *Astron. and Astrophys.*, 481, 337
- Kuijken, K., Fisher, D., & Merrifield, M. R. 1996, *Monthly Notices Roy. Astron. Soc.*, 283, 543
- Larson, R. B., Tinsley, B. M., & Caldwell, C. N. 1980, *Astrophys. J.*, 237, 692
- Laurikainen, E., Salo, H., Athanassoula, E., et al. 2013, *Monthly Notices Roy. Astron. Soc.*, 430, 3489
- Laurikainen, E., Salo, H., Buta, R., Knapen, J. H., & Comerón, S. 2010, *Monthly Notices Roy. Astron. Soc.*, 405, 1089
- Le Borgne, D., Rocca-Volmerange, B., Prugniel, P., et al. 2004, *Astron. and Astrophys.*, 425, 881
- Lequeux, J., Peimbert, M., Rayo, J. F., Serrano, A., & Torres-Peimbert, S. 1979, *Astron. and Astrophys.*, 80, 155
- MacArthur, L. A., Courteau, S., & Holtzman, J. A. 2003, *Astrophys. J.*, 582, 689
- Makarov, D., & Karachentsev, I. 2011, *Monthly Notices Roy. Astron. Soc.*, 412, 2498
- Makarov, D. I., & Karachentsev, I. D. 2009, *Astrophysical Bulletin*, 64, 24
- Méndez-Abreu, J., Aguerri, J. A. L., Corsini, E. M., & Simonneau, E. 2008, *Astron. and Astrophys.*, 478, 353
- Moore, B., Katz, N., Lake, G., Dressler, A., & Oemler, A. 1996, *Nature*, 379, 613
- Naim, A., Lahav, O., Buta, R. J., et al. 1995, *Monthly Notices Roy. Astron. Soc.*, 274, 1107
- Osterbrock, D. E., & Ferland, G. J. 2006, *Astrophysics of gaseous nebulae and active galactic nuclei*
- Pettini, M., & Pagel, B. E. J. 2004, *Monthly Notices Roy. Astron. Soc.*, 348, L59
- Quilis, V., Moore, B., & Bower, R. 2000, *Science*, 288, 1617
- Reshetnikov, V., & Sotnikova, N. 1997, *Astron. and Astrophys.*, 325, 933
- Roškar, R., Debattista, V. P., Brooks, A. M., et al. 2010, *Monthly Notices Roy. Astron. Soc.*, 408, 783
- Rubin, V. C., Ford, Jr., W. K., & Whitmore, B. C. 1984, *Astrophys. J. Let.*, 281, L21
- Schlegel, D. J., Finkbeiner, D. P., & Davis, M. 1998, *Astrophys. J.*, 500, 525
- Sil'chenko, O. K., Proshina, I. S., Shulga, A. P., & Kuposov, S. E. 2012, *Monthly Notices Roy. Astron. Soc.*, 427, 790
- Spitzer, Jr., L., & Baade, W. 1951, *Astrophys. J.*, 113, 413
- Sulentic, J. W., Verdes-Montenegro, L., Bergond, G., et al. 2006, *Astron. and Astrophys.*, 449, 937
- Thomas, D., Maraston, C., & Bender, R. 2003, *Monthly Notices Roy. Astron. Soc.*, 339, 897
- Trager, S. C., Faber, S. M., Worthey, G., & González, J. J. 2000, *Astron. J.*, 120, 165
- Tremonti, C. A., Heckman, T. M., Kauffmann, G., et al. 2004, *Astrophys. J.*, 613, 898